

Characterizing the Spatial Pattern Changes of Urban Heat Islands in Metro Manila Using Remote Sensing Techniques

Rosalyn A. Pereira* and Epifanio D. Lopez

*Department of Geodetic Engineering
University of the Philippines Diliman
Quezon City 1101 PHILIPPINES*

ABSTRACT

This study characterizes the spatial pattern of urban heat island (UHI) phenomenon when *in situ* measurements are not available. Images obtained from remote sensors operating in the thermal infrared wavelength of Landsat Thematic Mapper (TM) and Enhanced Thematic Mapper (ETM+) were used to derive the surface temperature of Metro Manila from 1989 to 2002; thereon, the formation of urban surface heat islands became apparent. The impact of urbanization to surface urban temperature is noticeable— the average annual rate of urban growth is found to be 1.33 percent while the rise of UHI has an annual growth rate of 0.8 degrees Celsius. Likewise, increase in land surface temperature is related to the decrease in leaf biomass. These were evident from changes in land cover parameters such as fractional vegetation cover and surface moisture availability. These parameters were derived by computing the normalized difference vegetation index (NDVI) from the images.

1. INTRODUCTION

Urbanized areas consist of built environment which have surfaces with low reflectivity Estes [5]. The non-transpiring materials of the built environment have higher thermal storage capacity than natural surfaces. Urban built-up have high solar radiation absorption and greater thermal capacity Weng et. al [35] that generate a higher amount of anthropogenic heat Streutker [28]. The removal of natural vegetation and replacement of low-reflective, non-evaporating and non-transpiring surfaces such as metal, asphalt and concrete has significant effects in the atmosphere Estes [5], Owen [23]; the unrestricted use of these materials modifies the local weather and climate Streutker [28], Voogt [33].

UHI has no direct effect on global warming since urban areas cover only 0.25 percent of the Earth's surface area Voogt and Oke [33]. Nevertheless global effects such as greenhouse gas emissions occur due to increased energy use as demand for air conditioning and cooling purposes increased Voogt [32], Taha [29], Murdiyarso [22], and Weng [36].

*Correspondence to: Department of Geodetic Engineering
University of the Philippines Diliman
Quezon City 1101 PHILIPPINES

Weng et al. [35] and Voogt and Oke [33] describe two types of UHI known as the urban canopy layer heat islands and the urban boundary layer heat islands where the former is situated just below the latter and is influenced by urban surface. Most UHI studies are conducted using extensive *in situ* measurements of air temperatures with the advantage of long data record, but these have poor spatial extent Streutker [28]. With the advent of technology, satellite remote sensing plays a major role in observing surface UHI Weng et al. [35] 2004; Streutker [28]; Voogt [32] 2002, for having a higher spatial distribution and uniform sampling of large number of data points than *in situ* measurements Streutker [28]. It can also give access to global and uniform estimates of surface temperature but has shorter data record Kerr et al. [17]. Satellite sensors detect radiation emitted and reflected by the surfaces on the earth, and with the use of image processing techniques such as radiometric and atmospheric correction, the apparent surface temperature can be derived Fukui [10]. The satellite-derived radiant surface temperature is called land surface temperature (LST) and is often referred to as surface urban heat island Voogt and Oke [33]. LST closely corresponds to urban canopy layer heat islands Weng et al. [35].

Recent studies utilize the thermal sensor of the Landsat Thematic Mapper and Enhanced Thematic Mapper Plus (TM/ETM+) to examine the spatial distribution of urban thermal pattern. The combination of the urban surface characteristics and land use maps to describe the activities occurring in the urban surface has been applied in the works of Shaikh et al. [26] in Nagasaki, Japan and Kangnung, South Korea, Weng [34] in Zhujiang Delta, China and Lougeay et al. [19] in Phoenix, Arizona.

Another application using the same sensor assesses the thermal behavior of urban surfaces in relation to biophysical parameters of the surface characteristics such as fraction vegetation cover (Fr) and surface moisture availability (M_0) through the technique known as Normalized Difference Vegetation Index (NDVI). Similar studies are conducted by Jo et al. [14] in Seoul, Korea, Hung and Yasuoka [13] in Hochi Minh City, Vietnam, Kustas and Albertson [18] in Arizona, and Weng and Yang [36] in Guangzhou City, China.

In the Philippines, literature on urban temperature relating to urbanization are very few; limitations due to data availability and difficulties in data gathering might be two of the primary reasons for this. All related studies have been conducted using *in situ measurements*. For instance, Estoque and Sta. Maria (2000) observed air temperature and rainfall in two weather stations of PAG-ASA in Metro Manila while Cruz and Villarín [4] conducted a twenty-day simulation using air temperature, wind direction and land cover maps available from PAG-ASA. In collaboration with the Japanese government (JICA Foundation), Hoyano et al. [12] also computed for 'Heat Island Potential' to evaluate the thermal environment of Metro Manila urban blocks.

The first objective of this study is to derive the pattern of UHI in an urban area over a thirteen-year period from 1989 to 2002. Since satellite-derived data is measured in radiance, this study focused on the surface temperature heat island and not on the air temperature heat island. The second objective is to derive the relevance of the surface characteristics with urban climate by adapting the works of Gillies and Carlson [11], Owen et al. [23], and Hung and Yasuoka [13] using the "triangle method" - a scatterplot of vegetation cover and surface radiant temperature (T_s) for satellite remotely-sensed pixels to show the extent of a complete range of surface radiant temperature and vegetation cover. This method also detects land cover alterations due to urbanization Voogt and Oke [33].

Although the use of remote sensing has its advantages, several considerations must be

Sensor Type	Landsat 4 TM	Landsat 5 TM	Landsat 7 ETM+
Path/Row	116/050	116/050	116/050
Acquisition Date	25-Jan-89	2-Apr-93	4-Mar-02
Pseudo-color scheme	RGB (band 4,3,2)	RGB (band 4,3,2)	RGB (band 4,3,2)
Source	UP Department of Geodetic Engineering	Global Land Cover Facility University of Maryland	Global Land Cover Facility University of Maryland

Table I. Landsat images and their sources

made in studying the urban heat island effect. One must be aware that satellite-derived temperature measurements are surface temperatures of the emitting materials. In contrast, *in situ* measurements are often air temperatures. Since surface types of the urban environment are varied, surface temperature exhibits greater spatial variation than the concurrent air temperatures Streutker [27]. Since surface types of the urban environment are varied, surface temperature exhibits greater spatial variation than the concurrent air temperatures Streutker [27].

2. THE STUDY AREA

Metro Manila was chosen for this study due to its large area and rapid urban growth over the past two decades. Vinluan et al. [31]. It is the capital of the Philippines and has an area of 636 km^2 composed of 13 cities and 4 municipalities (Figure 1). Major developments in Metro Manila were vigorously promoted during the past decade to bring the country into a newly industrialized economy Kelly [16]. It is now considered as one of the *megacities* in the world Vinluan et al. [31]. In 2000, its population increased to 10 million residents, which is more than 12 percent of the whole country; its birth rate of 2.5 percent is one of the highest in the world Vinluan et al. [31].

3. MATERIALS AND METHODS

3.1. The Available Data

Three Landsat images were used as primary data for measuring and detecting UHI between 1989, 1993 and 2002 (Table I).

Metro Manila, Philippines

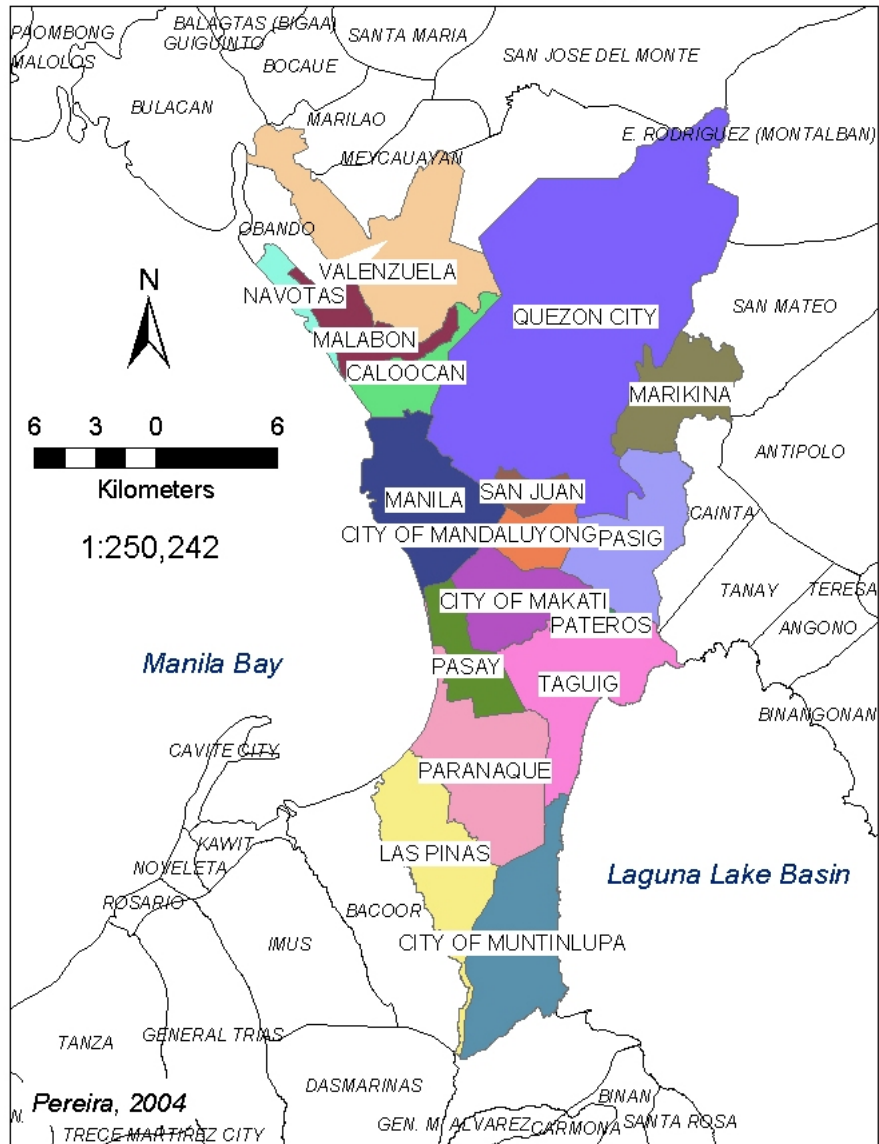


Figure 1. Metro Manila composed of 13 cities and 4 municipalities

3.2. Preprocessing of Landsat Images

The satellite images were rectified with the image processing software Environment for Visualizing Images (ENVI) version 3.6 using ground control points (GCPs) established by Global Positioning Systems (GPS) using handheld GPS receivers. The UTM - zone 51 coordinates in the Luzon Datum were used for geo-referencing. GCPs with root-mean-square error (RMSE) greater than 15 meters or more than one-half the pixel size were discarded. Image warping was done using polynomial function and the nearest neighbor resampling method. Nearest neighbor resampling uses the nearest pixel without any interpolation to create the warped image. The Metro manila boundary data was imported with the same georeferenced coordinates as the satellite images to serve as the basis for sub-setting. Digital Numbers (DN) were converted to absolute radiance values in the image using the following equation:

$$L = (DN - Bias)/Gain \quad (1)$$

where

- DN = digital number value recorded
- G = slope of response function (channel gain)
- L = spectral radiance measured
- B = intercept of response function (channel offset)

Further image enhancement was applied using gray-level thresholding with binary mask of clouds.

3.3. Land Cover Classification

The land cover classes was adopted from the works of Vinluan et al. [31] and the detailed methodology can be seen in the thesis study by Pereira [24].

Supervised classification using the maximum likelihood method was used in identifying land cover types. The accuracy of the classification result was derived by comparing the result of the classification with the ground truth information that was randomly gathered throughout the study area Vinluan et al. [31].

3.4. Land Surface Temperature Extraction

Surface temperature was extracted from the thermal image data and applied the appropriate band ratio algorithm on the infrared bands using the USGS thermal band algorithm. The isopleth map was extracted from band 6L of the Landsat satellite images. The thermal band was first converted from DN to at-satellite radiance using equation (2), and then to effective at-satellite temperature (T) using equation (3):

$$L = Bias + (Gain * DN) \quad (2)$$

$$T = K_2 / \ln(K_1 / L + 1) \quad (3)$$

where

- T = effective at-satellite surface temperature in Kelvin
- K_1 = calibration constant 1 (refer to nomenclature, p.29)
- K_2 = calibration constant 2 (refer to nomenclature, p.29)
- L = spectral radiance in watts/(meter² *ster*micro m)

3.5. Image Transformation - derivation of NDVI

Normalized Difference Vegetation Index (NDVI) was applied to transform the multispectral data into a single image band representing vegetation distribution. The NDVI values indicate the amount of green vegetation present in the pixel. NDVI is the algebraic combination of surface radiance in the red spectral band (0.56 to 0.68 μm) and near-infrared spectral band (0.75 to 1.1 μm) in the satellite image.

$$NDVI = (NIR - R)/(NIR + R) \quad (4)$$

where

- $NDVI$ = Normalized Difference Vegetation Index
- NIR = near-infrared spectral band
- R = red spectral band

3.6. Derivation of the 'triangle' scatterplot

NDVI and LST results were normalized ($NDVI^*$) and (T^*). Carlson and Arthur [2] defined the relationship between NDVI and fractional vegetation cover (Fr) in the following equation:

$$Fr = N^{*2} \quad (5)$$

N^* 's vary from 0 to 1 where and N^* equal to zero is represented as bare soil and N^* equal to 1 is represented as full vegetation cover. Normalization procedure was carried out using equations 6 and 7 to correct for interscene variability and phenology of the surface and conditions of the vegetation and atmosphere, i.e., haze, wind speed and humidity Owen et al. [23]. The normalization of NDVI and temperature was necessary to compare data from the three different images.

$$NDVI^* = (NDVI - NDVI_{low})/(NDVI_{high} - NDVI_{low}) \quad (6)$$

$$T^* = (T - T_{low})/(T_{high} - T_{low}) \quad (7)$$

4. RESULTS AND DISCUSSION

4.1. Urban growth pattern

Urban growth in Metro Manila increased from 64 percent built-up cover in 1989 to 67 percent in 1993 and 79 percent in 2002. In 1989, the urban core was located in the central district of

MUNICIPALITIES	1989	1993	2002
CALOOCAN	83%	92%	98%
CITY OF MAKATI	83%	75%	93%
CITY OF MANDALUYONG	82%	78%	87%
CITY OF MUNTINLUPA	32%	58%	61%
LAS PINAS	42%	69%	81%
MALABON	60%	66%	76%
MANILA	92%	91%	95%
MARIKINA	65%	58%	79%
NAVOTAS	24%	25%	27%
PARANAQUE	49%	74%	85%
PASAY	74%	73%	92%
PASIG	76%	70%	87%
PATEROS	95%	63%	88%
QUEZON CITY	45%	59%	71%
SAN JUAN	93%	88%	96%
TAGUIG	57%	47%	71%
VALENZUELA	33%	50%	64%
TOTAL	64%	67%	79%

Table II. Built-up cover in Metro Manila (1989-2002)

Metro Manila. Ten cities had more than 60 percent built-up areas, which included the cities of Caloocan, Makati City, Mandaluyong City, Malabon, Marikina, Pasay, Pasig, Pateros and San Juan. By 1993, Las Pinas and Paranaque were also more than 60 percent built-up. By 2002, the rest of Metro Manila had more than 60 percent built-up cover except for Navotas (Table II).

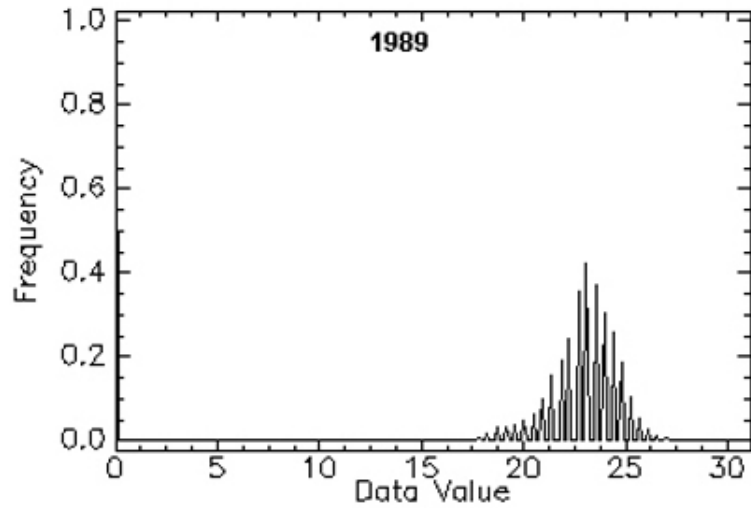
The average annual rate of urban growth in Metro Manila was 0.75 percent per year from 1989 to 1993 and 1.33 percent per year from 1993 to 2002. The population growth rate in Metro Manila has decreased during the last two decades, human settlement have been spreading out of Metro Manila toward its adjacent municipalities as space has become a limiting factor for urban growth Vinluan et al. [31]; Moriwake et al. [21](Table III).

4.2. Land Surface Temperature Analysis

The mean land surface temperature (MLST) for Metro Manila in 1989 stood at 22.5 degrees Celsius \pm 1.86, while it was 29.3 degrees Celsius \pm 2.20 in 1993 and 32.9 degrees Celsius \pm 2.92 2002. This shows in an annual rate of increase at 0.8 degrees Celsius per year (Figure 2-4).

Mean land surface (MLST) was also computed for each municipality in Metro Manila from 1989 to 2002 (Table IV) to determine the concentration of heat islands within Metro Manila. Results show increasing LST magnitude in degrees Celsius within the thirteen-year period across the thirteen municipalities of Metro Manila (Figure 5).

In 2002 (Table IV), Caloocan has the highest recorded mean land surface temperature of 34.4 degrees Celsius; it is a residential and industrial suburb for shoes and other consumer items in Metro Manila. While Navotas having the lowest recorded mean land surface temperature



1989 Land Surface Temperature Profile in Metro Manila

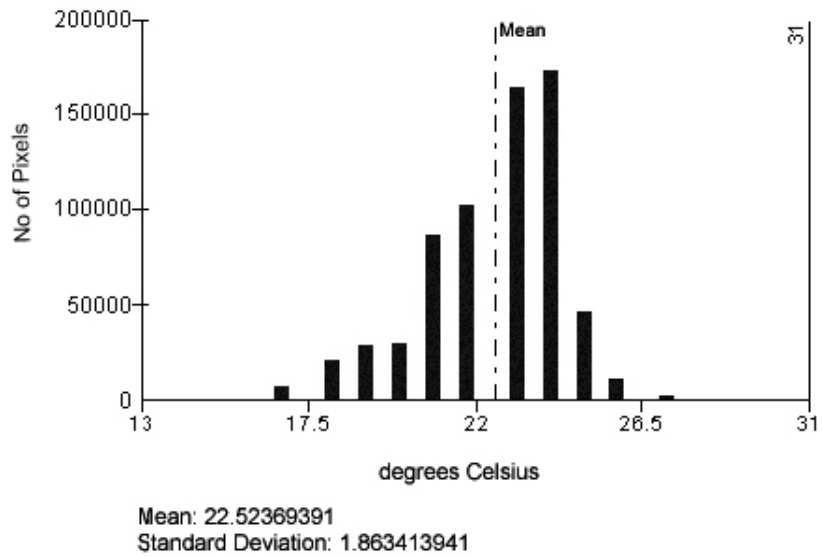
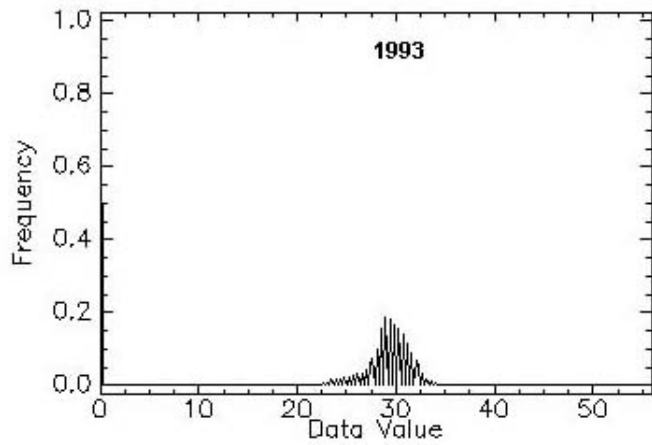


Figure 2. Number of pixels versus land surface temperature in 1989



1993 Land Surface Temperature Profile in Metro Manila

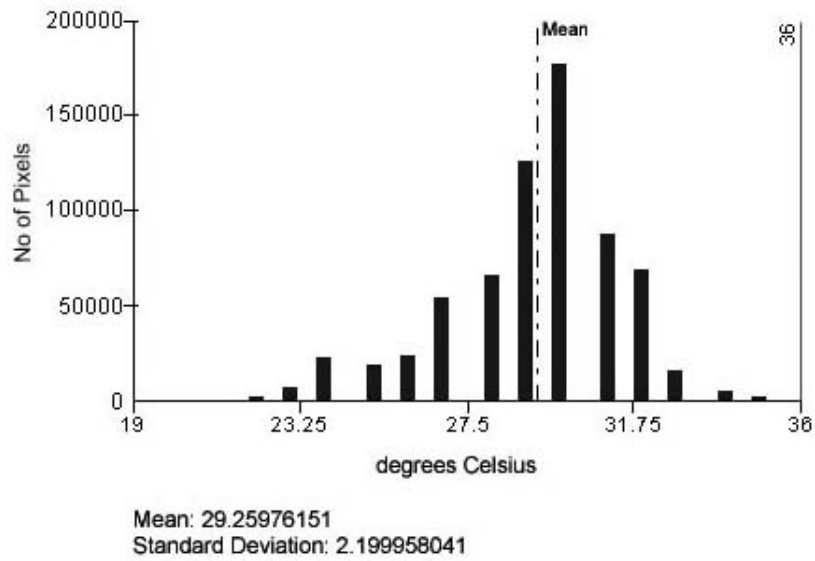
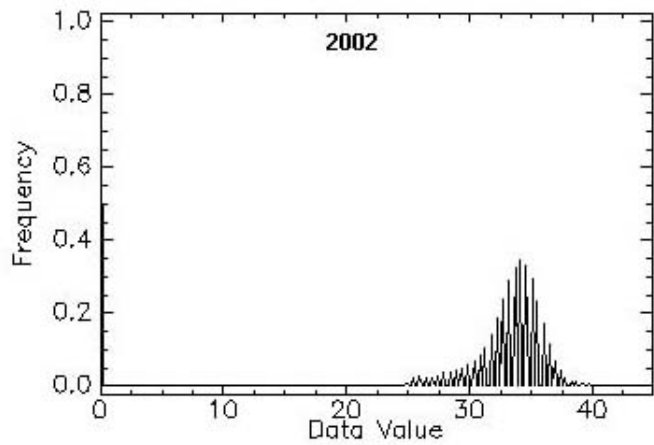


Figure 3. Number of pixels versus land surface temperature in 1993



2002 Land Surface Temperature Profile in Metro Manila

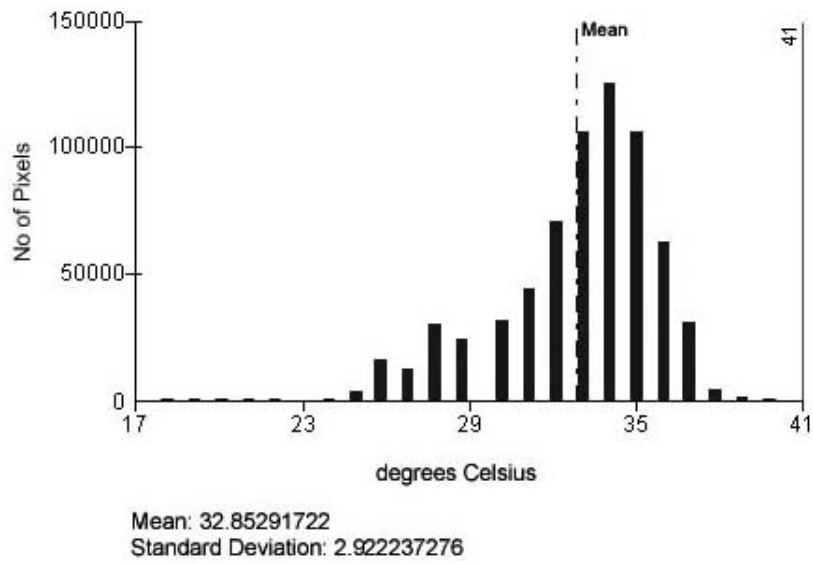


Figure 4. Number of pixels versus land surface temperature in 2002

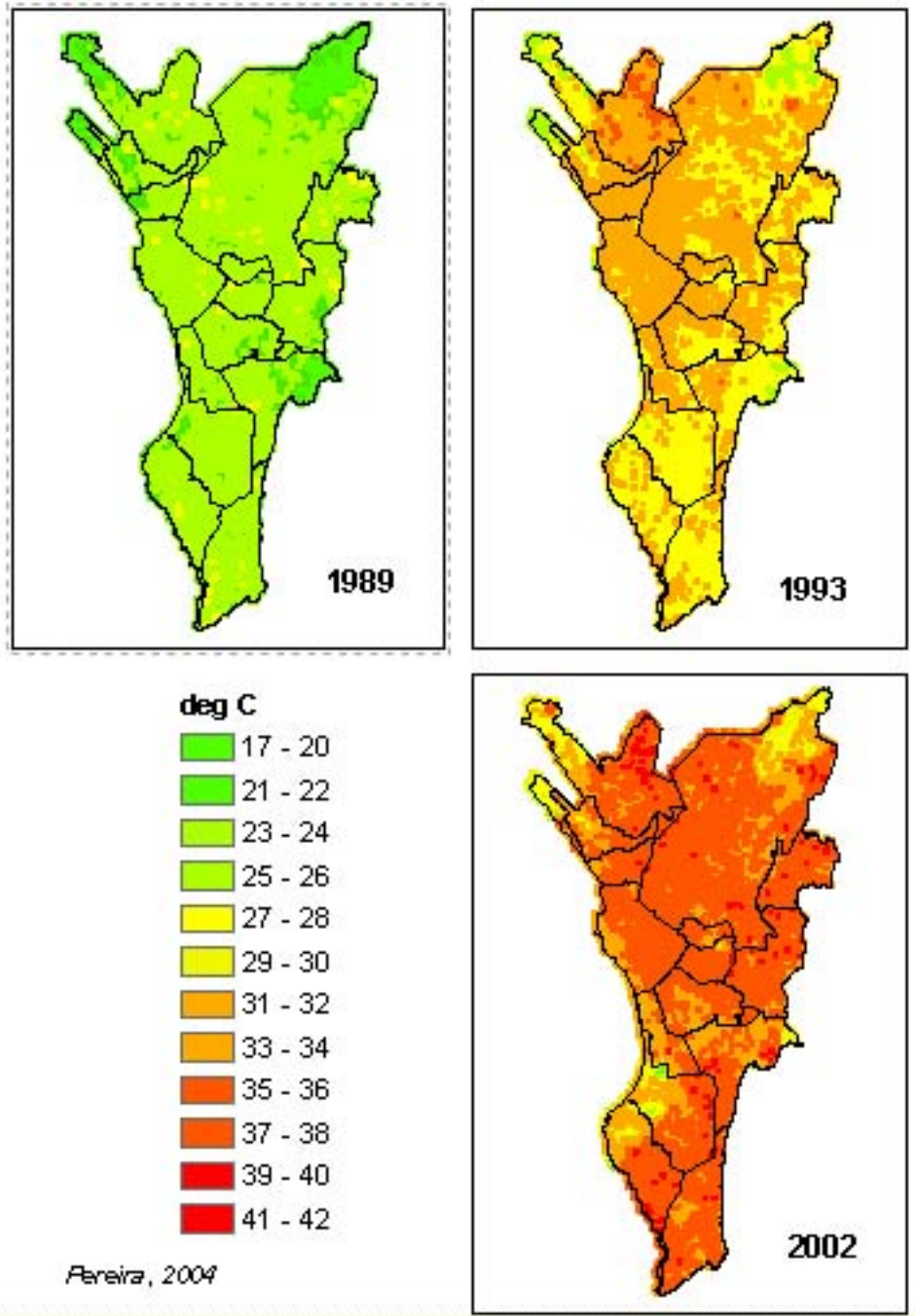


Figure 5. Land surface temperature in Metro Manila from 1989 to 2002

MUNICIPALITIES	1990	1995	2002
CALOOCAN	763,414	1,023,159	1,177,604
CITY OF MAKATI	453,170	484,176	444,867
CITY OF MANDALUYONG	248,143	286,870	278,474
CITY OF MUNTINLUPA	278,411	399,846	379,310
LAS PINAS	297,102	413,086	472,780
MALABON	280,027	347,484	338,855
MANILA	1,601,237	1,654,761	1,581,082
MARIKINA	310,227	357,231	391,170
NAVOTAS	187,479	229,039	230,403
PARANAQUE	308,236	391,296	449,811
PASAY	368,366	408,610	354,908
PASIG	397,679	471,075	505,058
PATEROS	51,409	55,286	57,407
QUEZON CITY	1,669,776	1,989,419	2,173,831
SAN JUAN	126,854	124,187	117,680
TAGUIG	266,637	381,350	467,375
VALENZUELA	340,227	437,165	485,433
TOTAL	7,948,395	9,454,040	9,906,048

Source: National Statistics Office (1990, 1995, 2000)

Table III. Population of Metro Manila (1990-2000)

of 27.6 Celsius is the fishing center of Metro Manila.

Land surface temperature profile was superimposed with urban growth in Metro Manila and showed the relevant increase of mean land surface temperature caused by increasing built-up cover from 1989 to 2002 (Figure 6).

4.3. The Triangle Method

The scatterplot resembles a truncated triangle where the radiant surface temperature was represented by the relative amounts of bare surface and vegetation as seen by the sensor, as well as surface moisture conditions Arthur-Hartranft et al. [1]. A triangle was formed since surface temperature has little spatial variation over dense vegetation but large spatial variation over bare soil surfaces Carlson and Arthur [2].

The darkened right edge is the 'warm edge.' $NDVI_{low}$ is the base of the triangle assumed to have zero surface soil water content and defines the base of the triangle while $NDVI_{high}$ assumes it has reached 100 percent vegetation cover. T_{max} is the intersection of the "warm edge" and $NDVI_{low}$ while T_{min} is the representative of canopy temperature.

The plot also shows the extent of the complete range of surface radiant temperature and vegetation cover surface soil moisture availability (surface soil water content) values (M_o) (Figures 7-9).

The scatterplots of radiant surface temperature versus NDVI for 1989, 1993 and 2002 reveal that built-up cover has increased in surface temperature and was accompanied by a relevant decrease in leaf biomass index while an inverse relation holds true for the surface temperature

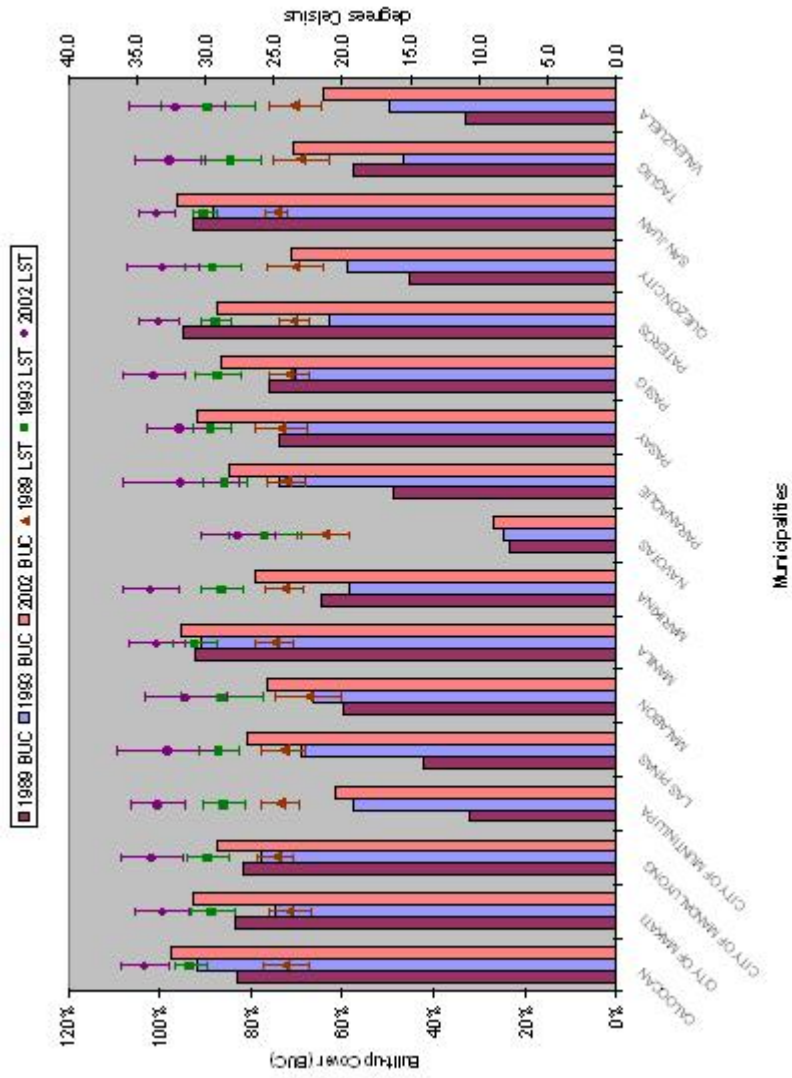


Figure 6. Profile of mean land surface temperature versus built-up cover

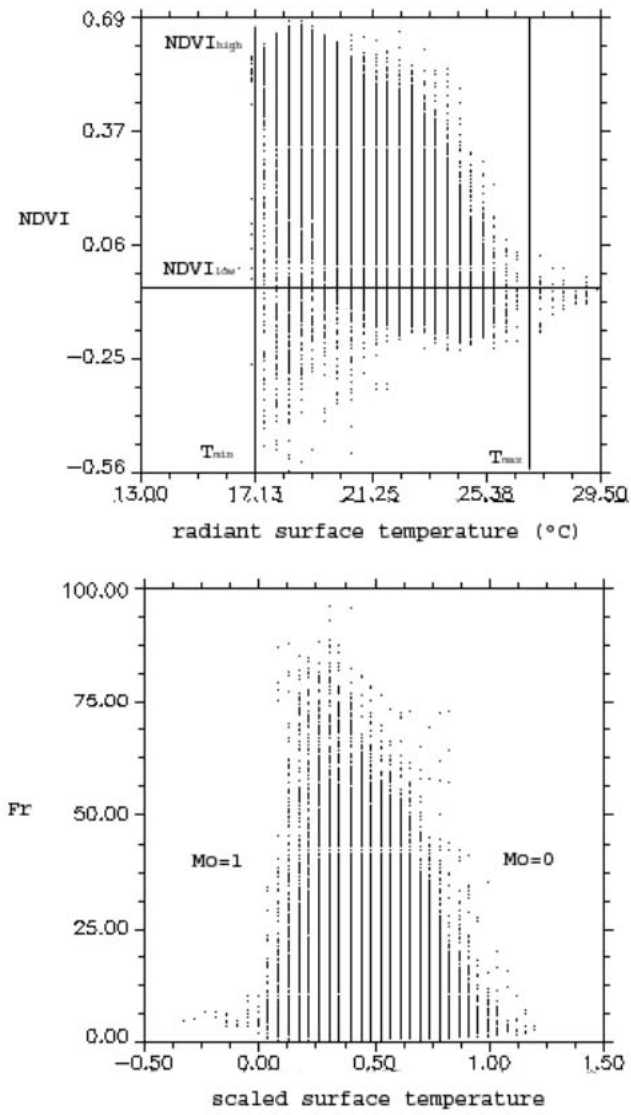


Figure 7. 1989 Scatterplot of NDVI versus radiant surface temperature

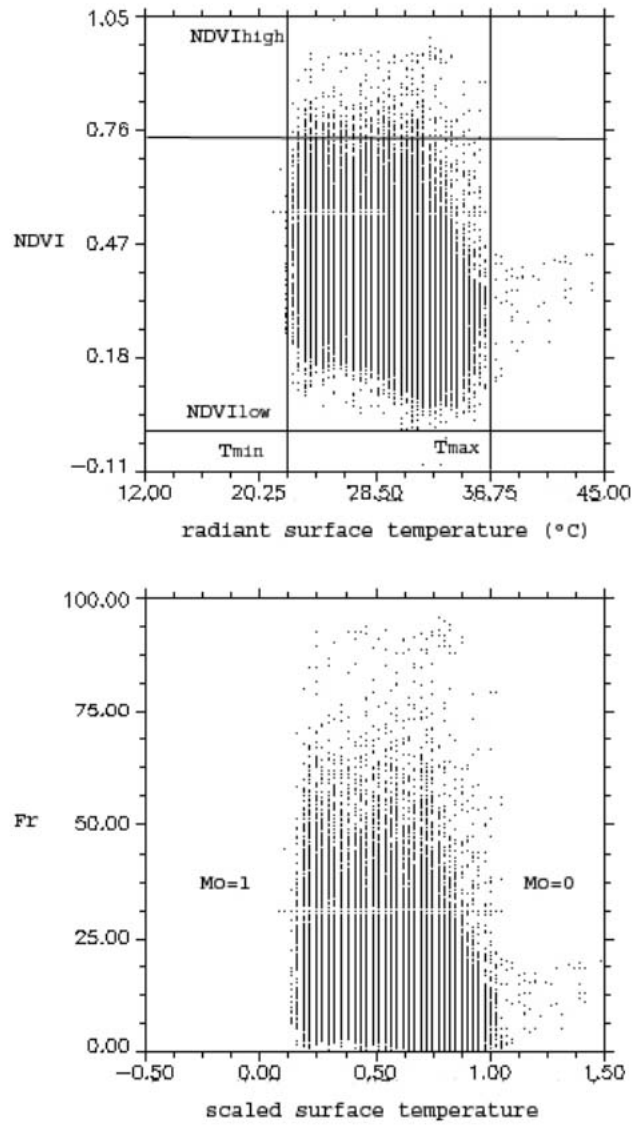


Figure 8. 1993 Scatterplot of NDVI versus radiant surface temperature

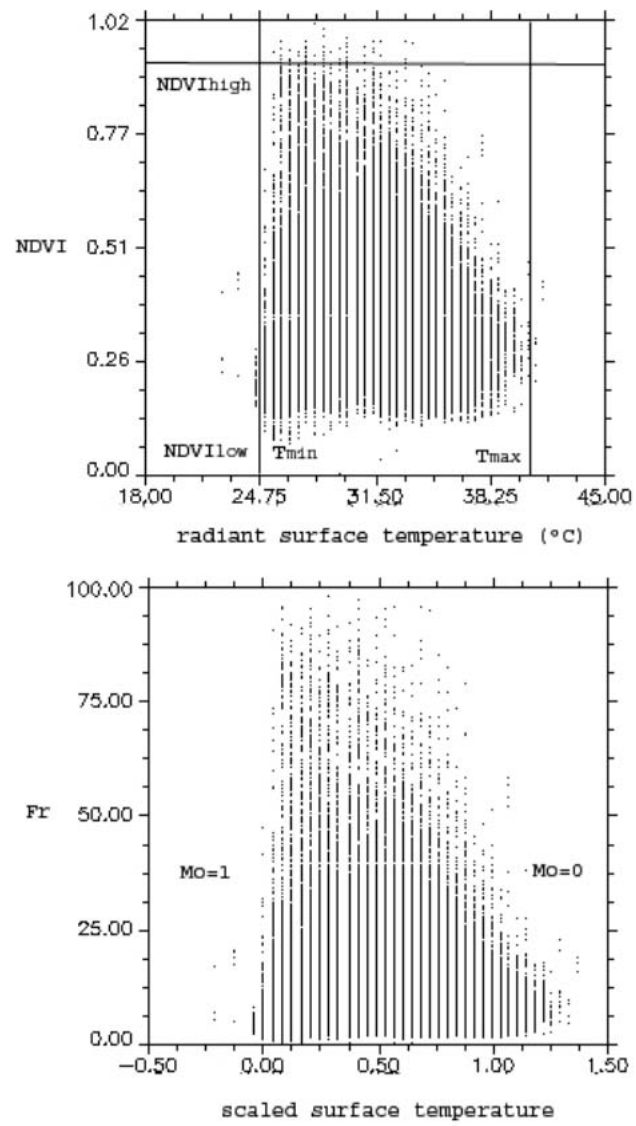


Figure 9. 2002 Scatterplot of NDVI versus radiant surface temperature

MUNICIPALITIES	1989	1993	2002	Δ 1989-1993	Δ 1989-2002
	°C				
CALOOCAN	24.1	31.1	34.4	6.9	10.2
CITY OF MAKATI	23.9	29.5	33.1	5.6	9.2
CITY OF MANDALUYONG	24.8	29.8	33.9	4.9	9.0
CITY OF MUNTINLUPA	24.5	28.6	33.4	4.1	8.9
LAS PINAS	24.3	29.0	32.7	4.7	8.4
MALABON	22.4	28.8	31.4	6.3	9.0
MANILA	25.0	30.7	33.5	5.8	8.6
MARIKINA	24.2	28.8	34.0	4.6	9.8
NAVOTAS	21.4	25.6	27.6	4.3	6.2
PARANAQUE	24.1	28.5	31.8	4.5	7.7
PASAY	24.5	29.5	31.8	5.5	7.4
PASIG	23.9	29.0	33.7	5.1	9.8
PATEROS	23.6	29.2	33.4	5.6	9.8
QUEZON CITY	23.4	29.4	33.1	6.0	9.6
SAN JUAN	24.8	30.1	33.5	5.2	8.7
TAGUIG	23.0	28.1	32.6	5.1	9.6
VALENZUELA	23.5	29.8	32.1	6.3	8.6

Table IV. Mean Land Surface Temperature in Metro Manila (1989-2002)

and vegetation cover. Pixels that have high percentage in the urbanized area correspond to low fractional vegetation cover (Fr) and surface moisture availability (M_o). This behavior suggests an increase in sensible heat flux due to decrease in vegetation cover and increase of non-evaporating, non-transpiring surfaces Owen et al. [23].

A large percentage of built-up areas in Metro Manila is impervious to moisture, hence moisture availability in Metro Manila decreases proportionately with the decrease in vegetation cover. Urbanized areas have lower albedo (reflectivity) which is caused by the use of materials such as asphalt roadways, metals and concrete. The non-transpiring materials of the built environment have higher thermal storage capacity than natural surfaces.

5. CONCLUSIONS

Urban growth has brought with it corresponding increase in land surface temperature. In Metro Manila, increase in built-up cover has direct effect on the aggravation of the heat island effect. Remote sensing is useful in detecting the presence of UHI. The change in spatial pattern from urban expansion is correlated with the increasing spatial pattern change of UHI, while the increase in land surface temperature is related to the decrease in leaf biomass and decrease in surface moisture availability. Urban heat islands (UHI) can be effectively mitigated by the reduction of urban built-up cover. However, since this process is not realistically possible due to the natural human predilection to urbanization, vegetation cover may then be increased to compensate for the adverse effect of UHI.

REFERENCES

1. Arthur-Hartranft, S.T., Carlson, T.N. and Clarke, K.C. (2003). Satellite and ground-based micro climate and hydrologic analyses coupled with a regional urban growth model. *Remote Sensing of Environment*, 86:385-400.
2. Carlson, T.N. and Arthur, S.T. (2000). The impact of land use - land cover changes due to urbanization on surface microclimate and hydrology: a satellite perspective. *Global and Planetary Change*, 25: 49-65.
3. Comrie, A.C. (2000). Mapping a Wind-Modified Urban Heat Island in Tucson, Arizona, *Bulletin of the American Meteorological Society*, 2417 - 2431.
4. Cruz, F.T. and Villarin, J.T. (2003). Changes in the Surface Temperature and Winds due to the Growth of the Metro Manila Urban Area. *Samahang Pisika ng Pilipinas 2003 Congress Proceedings*.
5. Estes, M. Jr. Quattrochi, and Stasiak. year.(1999). The Urban Heat Island Phenomenon: How its effects can influence environmental decision making in your community. *1999 National Planning Conference*.
6. Estoque, M.A. and Sta. Maria, M.V. (2000). Climate Changes due to the Urbanization of Metro Manila. *Manila Observatory Scientific Report No. 3*.
7. Dousset B. and Gourmelon, F. (2003). Satellite multi-sensor data analysis of urban surface temperatures and landcover. *Journal of Photogrammetry and Remote Sensing*, 58: 43-54.
8. Deosthali, V. (2000). Impact of rapid urban growth on heat and moisture islands in Pune City, India. *Atmospheric Environment*, 34: 2745-2754.
9. Fernandez, F., Montavez, J., Gonzalez-Rouco, F. and Valero, F. (2003). A PCA Analysis of the UHI Form of Madrid. *International Conference on Urban Climate*, September 1-5, 2003.
10. Fukui, Y. (2003). A Study on Surface Temperature Patterns in the Tokyo Metropolitan Area Using ASTER Data. *Proceedings of Asian Conference on Remote Sensing and 2003 International Symposium on Remote Sensing*, 843-845.
11. Gillies, R.R., and Carlson, T.N. (1995). Thermal remote sensing of surface soil water content with partial vegetation cover for incorporation into climate models. *Journal of Applied Meteorology*, 34: 745-756.
12. Hoyano, A., Lino A., Yoon, S. (2002) Toward Creating a "Sustainable City" Metro Manila: In Search of Sustainable Future edited by Ohmachi, T. and Roman, E. University of the Philippines Press, Manila, 223-228.
13. Hung, T. and Yasuoka, Y. (2002). Remote Sensing to analyze the changes of surface biophysical parameters in Vietnam's urbanized area. *The 23rd Asian Conference on Remote Sensing, Kathmandu, Nepal*, Nov. 25-29, 2002.
14. Jo, M.H. (2003). Analyzing the Correlation between Urban Forestry and Surface Temperature Using Landsat TM data. *Proceedings of Asian Conference on Remote Sensing and 2003 International Symposium on Remote Sensing*, 618-620.
15. Kawashima, S., Tomoyuki, I., Mitsuo, M. and Tetsuhisa, M. (2000). Relations between surface temperature and air temperature on a local scale during winter nights. *Journal of Applied Meteorology*, 39(9): 1570-1579.
16. Kelly, P.F. (1998). The politics of urban-rural relations: Land use conversion in the Philippines. *Environment and Urbanization Journal*, 10(1):35-54.
17. Kerr, Y.H., Lagourde, J.P. and Imbernon, J. (1992). Accurate land-surface temperature retrieval from AVHRR data with the use of an improved split-window algorithm. *Remote Sensing of Environment*, 41:97-209.
18. Kustas, W.P., and Albertson, J.D. (2003). Effects of surface temperature contrast on land-atmosphere ex-change: A case study from Monsoon 90. *Water Resource Res.*, 39(6).
19. Lougeay, R., Brazel, A., and Hubble, M. (1996). "Monitoring Intra Urban Temperature Patterns and Associated Land Cover in Phoenix, Arizona Using Landsat Thermal Data." *Geocarto International* 11(4):79-89
20. McKendry, I.G., Oke, T.R., Klysik, K. and Fortuniak, K. (2001). Application of Neural Networks to Urban Heat Island studies in Lodz, Poland. *Urban Meteorology - Oral Programme*, March 26, 2001.
21. Moriwake, M., Palijon, A. and Takeuchi, K. (2002). Distribution and structure of urban green spaces in Metro Manila. Metro Manila: In search of a sustainable Future edited by Ohmachi, T. and Roman, E.R., University of the Philippines Press, Manila, 185-198.
22. Murdiyarso, D. and Wasrin, U.R. (1995). Estimating land use change and carbon release from tropical forest conversion using remote sensing technique. *Journal of Biogeography*, 22: 715-721.
23. Owen, T.W., Carlson, T.N., and Gillies, R.R. (1998). An assessment of satellite remotely-sensed land cover parameters in quantitatively describing the climatic effect of urbanization. *International Journal of Remote Sensing*, 19: 1663-1681.

24. Pereira, R.A. (2004). Monitoring urban heat island phenomenon in Metro Manila, Philippines: A Remote Sensing-GIS Approach. MS Thesis. University of the Philippines.
25. Saaroni, H., Ben-Dor, E., Bitan, A. and Potcher, O. (2000). Spatial distribution and microscale characteristics of the urban heat island Tel-Aviv, Israel. *Landscape and Urban Planning*, 48: 1-18.
26. Shaikh, A. (2003). Land Surface Change Detection in Nagasaki and Kangnung using Multi-temporal Landsat Data. *Proceedings of Asian Conference on Remote Sensing and 2003 International Symposium on Remote Sensing*, 727-729.
27. Streutker, D.R. (2002). A remote sensing study of the urban heat island of Houston, Texas. *International Journal Remote Sensing*. 23(13):2595-2608.
28. Streutker, D.R. (2003). Satellite-measured growth of the urban heat island of Houston, Texas. *Remote Sensing of Environment*, 85: 43-54.
29. Taha, H., Akbari, H., Rosenfeld, A. and Huang, J. (1988). Residential cooling loads and the urban heat islands: The effects of albedo. *Building and Environment*, 23(4): 271-283.
30. Tso, C.P. (1996). A survey of urban heat island studies in two tropical cities. *Atmospheric Environment*, 30:507-519.
31. Vinluan, R.N., Quiblat, C., Batadlan, B., Asilo, S., Santillanosa, R., Pereira, R., Macapinlac, O. and Menguito, M. (2003). Monitoring urban growth in Metro Manila using multitemporal satellite images. *Proceedings of Sian Conference on Remote Sensing and 2003 International Symposium on Remote Sensing*, 849-851.
32. Voogt, J.A. (2002). Urban Heat Island Causes and consequences of global environmental change "Encyclopedia of Global Environmental Change" edited by Douglas, I., John Wiley and Sons, Inc. USA. 3: 660-666.
33. Voogt, J.A. and Oke, T.R. (2003). Thermal remote sensing of urban climate. *Remote Sensing of Environment*, 86:370-384.
34. Weng, Q. (2001). A remote sensing-GIS evaluation of urban expansion and its impact on surface temperature in the Zhujiang Delta, China. *International Journal of Remote Sensing*, 22: 1999-2014.
35. Weng, Q., Lu, D. and Schubring, J. (2004). Estimation of land surface temperature-vegetation abundance relationship for urban heat islands studies. *Remote Sensing of Environment*, 89: 467-483.
36. Weng, Q. and Yang, S. (2004). Managing the adverse thermal effects of urban development in a densely populated Chinese city. *Journal of Environmental Management*, 70: 145-156.

Symbol	Description	Equation	Unit
DN	Digital number value recorded	1	μm
G	Gain	1	μm
L	Spectral radiance measured	1	watts/(meter ² * ster * μm)
B	Bias	1	μm
T	Effective at-satellite temperature in Kelvin	3	
K_1	Calibration constant 666.09 (Landsat 7) 607.76 (Landsat 5)	3	watts/(meter ² * ster * μm)
K_2	Calibration constant 1282.71 (Landsat 7) 1260.56 (Landsat 5)	3	Kelvin
R	Surface radiance in the red band (0.56 to 0.68	6	μm
NIR	Surface radiance in the near-infrared band (0.75 to 1.1)	6	μm

Table V. Nomenclature

